Carrier-carrier interaction and ultrashort pulse propagation in a highly excited semiconductor laser amplifier beyond the rate equation limit

S. Hughes*
Semiconductor Optics Theory Group, Department of Physics, Washington State University, Pullman, Washington 99164-2814
(Received 25 November 1997)

The influence of carrier correlation processes on the interaction and propagation of femtosecond optical pulses in an inverted semiconductor is theoretically investigated. Microscopically treated Coulomb scattering described from a first-principles theory, including both diagonal and nondiagonal dephasing, is seen to cause considerably different behavior on the dynamics than that modeled by employing a rate-equation approximation. Semiconductor intrinsic optical nonlinearities such as gain saturation and adiabatic following, controlled by microscopic dephasing and relaxation mechanisms, manifest dominantly in ultrafast transient effects that, experimentally, can appear as a typical Kerr-type (instantaneous) nonlinearity. It is shown that one *cannot* invoke an adiabatic elimination for the polarization equation on femtosecond time scales. The present self-consistent theory successfully explains recent experimental measurements without recourse to parametrized equations. The possible role of non-Markovian relaxation is also discussed. [S1050-2947(98)10409-2]

PACS number(s): 42.55.−f

I. INTRODUCTION

The ultrafast dynamics in semiconductor optical amplifiers (SOA's) has been attracting considerable attention recently, due to the rapid developments in the field of semiconductor lasers [1]. Indeed, a plethora of semiconductor waveguide devices has amassed over the years, finding applications for smaller optical storage, ultrahigh-speed signal processing, laser printing, flat-panel displays, and more. From a theoretical viewpoint, the investigation of highly excited semiconductor media is also of intriguing interest because it is connected to Coulomb many-body processes such as excitonic effects and electron correlations [2]. The role of a first-principles microscopic theory is also desired for advising industries on optimal operating parameters. In order to accurately characterize and optimize the performance of SOA's, ultimately one has to understand the basic physical mechanisms to aid the development of semiconductor lasers. Experimentally this has involved injecting an ultrashort light pulse into the SOA and monitoring the dynamical response, for example, in excitation-probe [3,4] or four-wave-mixing [5] measurements. From these experimental measurements, there is evidence for ultrafast gain saturation effects, carrier heating, and spectral hole burning as well as for nonlinearities that act instantaneously.

The rate equation models (REM's) employed to explain the nonlinearities [3–5] are often in good agreement with experimental measurements. The appeal of the REM's, of course, lies in their conceptual simplicity and can include the phenomenological discussion of contributions of two-photon absorption (TPA) and free-carrier absorption (FCA) (see Ref. [4]). Nevertheless, despite its success, a shortcoming of the rate equation approach is that typically the occurring parameters are not microscopically determined and one can fit the data using a conglomeration of parameters that describe, phenomenologically, spectral hole burning, carrier heating, TPA, and FCA. For instance, in the rate equation approach TPA and FCA yield the ultrafast instantaneous response [4] observed in several experimental pump-probe studies.

Even if the REM's are very successful, the interaction of an electromagnetic light pulse with an inverted semiconductor is truly a many-body problem that cannot *a priori* be described by parametrized equations. From a microscopic point of view, the optical response of inverted semiconductors is determined by carrier-carrier and carrier-phonon interactions which today can be described within a parameter-free theory [2,6–8]. Also, REM's describe the light-matter interaction based on the assumption that the polarization varies instantaneously with the electric field (adiabatic approximation) that does not allow for the description of coherent effects. Moreover, recent four-wave-mixing (FWM) experiments have shown that the coherent response of a SOA can be resolved, even at room temperature [9], and therefore the adiabatic approximation cannot always be applied. A theoretical analysis of optical coherence in SOA's at a level that includes diagonal and nondiagonal dephasing agrees well with the FWM observations [10]. For comparison, the REM's in dye laser amplifiers have been shown to be invalid for optical pulses interacting with a material that has a polarization dephasing time on the order of the pulse duration [11], showing that beyond the rate equation approximation the pulse can develop a shoulder and pulse shortening occurs because of the finite coherence time. A similar observation of coherent propagation effects has also been reported for the SOA [12] and agrees with our propagation studies at the gain peak and the calculated dephasing times presented in this paper. Moreover, theoretical studies for coherent pulse propagation in extended samples indicate the possibility of femtosecond pulse breakup in the nonlinear and linear interaction regime [13,14]. Experimentally, pulse breakup in a fiber and semiconductor laser amplifier combined system has been observed [15] and is explained by the interplay of nonlinear properties and the gain dispersion of the amplifier that requires the inclusion of a frequency-dependent refractive

*Electronic address: shughes@wsu.edu

index and coherent effects not contained in the rate equation approach.

The purpose of the present paper is to present a self-consistent description of the ultrafast/coherent dynamics including the intrinsic nonlinearities in SOA's after the injection of a femtosecond pulse. For this purpose we study a two-band semiconductor model for the carriers and their Coulomb coupling without phenomenologically introduced parameters. In this context, our study may support or guide more phenomenological rate equation approaches. For the calculations we apply a numerical solution of generalized semiconductor Maxwell-Bloch equations [2,7,16–18]. In our approach, the carrier relaxation processes are treated on the level of quantum kinetic equations in the Markovian limit for the Coulomb interactions. The role of non-Markovian relaxation is also discussed. The influence of carrier-LO-phonon interactions occurs over much longer time scales than those studied in this paper and can be neglected.

This paper is organized as follows. After a review of the equations of motion we apply numerical solutions for two typical situations of interest. First, we discuss the temporal density and gain dynamics as a function of the photon energy. For this purpose, the amplifier is excited at the gain peak, near the transparency point, and in the aborbing regime where, within the method presented here, the gain dispersion and its intrinsic nonlinear dynamics is fully taken into account. This situation is typically studied in experiments where the pulses can be tuned over a wide spectral range. Second, we study the propagation dynamics of a femtosecond pulse at the peak gain of the amplifier where we discuss the cumulative influence of the optical nonlinearities on a propagating pulse profile. Both regimes are of relevance for the discussion of ultrafast optical experiments and applications in SOA's.

II. THEORETICAL APPROACH AND EQUATIONS OF MOTION

We assume a two-band bulk semiconductor where each electron-hole state with wave number k contributes to the total carrier density $N=2V^{-1}\Sigma_k f_k^{e/h}$. Here $f_k^{e/h}$ is the electron or hole carrier distribution and the factor of 2 accounts for the spin summation. In a similar manner the macroscopic polarization can be obtained from $P=2V^{-1}\Sigma_k d_{cv}(k)P_k$, where $d_{cv}(k)$ is the Kane dipole matrix element $d_{cv}(0)/\{1+E_g^{-1}[\varepsilon_e(k)+\varepsilon_h(k)]\}$, with E_g being the band-gap energy. Therefore, the polarization components P_k of each single-particle state k has to be computed. For our theoretical approach, we solve the semiconductor Bloch equations (SBE's) numerically and self-consistently treat the relaxation processes on the level of quantum kinetic equations in the Markovian limit. The SBE's [2,7,16–18] can be written as ($\hbar=1$)

$$\frac{\partial f_{\mathbf{k}}^{e/h}}{\partial t}=iP_{\mathbf{k}}^{\star}\Omega_{\mathbf{k}}-iP_{\mathbf{k}}\Omega_{\mathbf{k}}^{\star}+\left.\frac{\partial f_{\mathbf{k}}^{e/h}}{\partial t}\right|_{\mathrm{CC}}, \tag{1}$$

$$\frac{\partial P_{\mathbf{k}}}{\partial t}=-i\Delta_{\mathbf{k}}P_{\mathbf{k}}-i\Omega_{\mathbf{k}}(f_{\mathbf{k}}^{e}+f_{\mathbf{k}}^{h}-1)+\left.\frac{\partial P_{\mathbf{k}}}{\partial t}\right|_{\mathrm{CC}}, \tag{2}$$

where $\Delta_k=\varepsilon_k-\omega_l-\Sigma_q V_{k-q}(f_q^e+f_q^h)$ is the renormalized energy dispersion for a parabolic two-band semiconductor with unrenormalized transition energy $\varepsilon_k=(\frac{1}{2}m_e+\frac{1}{2}m_h)k^2+E_g$ and V_q is the Coulomb potential. The generalized Rabi frequency is $\Omega_k=d_{cv}(k)E+\Sigma_q V_{k-q}P_q$, where $E(z,t)$ is the slowly varying optical field propagating in the z direction (see below). Since the high-density regime in amplifiers is considered, Coulomb correlations between the carriers must be taken into account [$\dot{P}_k/\dot{f}_k|_{CC}$ contribution in Eqs. (1) and (2)]. The appropriate correlation contributions can be calculated within density matrix theory [16] or a Green's function method [17]. Within a screened second-order Born approximation in the Markovian limit, Coulomb correlations describe, on the one hand, carrier-carrier collisions resulting in a redistribution of carriers via in and out scattering of electron/hole occupations with the rates Γ_{in} and Γ_{out}. On the other hand, they yield diagonal $\Gamma_{\mathrm{d}}^{\mathrm{p}}$ as well as nondiagonal $\Gamma_{\mathrm{nd}}^{\mathrm{p}}$ contributions to the polarization dynamics, describing optical dephasing and corrections to the internal Hartree-Fock field.

The carrier-carrier scattering is calculated from the electron-hole Boltzmann equation under the inclusion of polarization scattering

$$\left.\frac{\partial f_{\mathbf{k}}^{a}}{\partial t}\right|_{\mathrm{CC}}=\Gamma_{\mathrm{in}}^{a,\mathrm{CC}}(\mathbf{k},f\,)(1-f_{\mathbf{k}}^{a})-\Gamma_{\mathrm{out}}^{a,\mathrm{CC}}(\mathbf{k},f\,)f_{\mathbf{k}}^{a}+(P_{\mathbf{k}}\Omega_{\mathbf{k}}^{*}|_{\mathrm{CC}}+\mathrm{c.c.})+(Q_{\mathbf{k}}^{*}+\mathrm{c.c.}), \tag{3}$$

where $\Gamma_{\mathrm{in},k}^{a,\mathrm{CC}}$ and $\Gamma_{\mathrm{out},k}^{a,\mathrm{CC}}$ ($a=e,h$) are the expressions for in and out scattering, for example;

$$\Gamma_{\mathrm{in}}^{a,\mathrm{CC}}(\mathbf{k},f\,)=4\sum_{\substack{\mathbf{k}',\mathbf{q}\\ b=e,h}}|W(\mathbf{q})|^2 f_{\mathbf{k}+\mathbf{q}}^{a}[(1-f_{\mathbf{k}'}^{b})f_{\mathbf{k}'-\mathbf{q}}^{b}]\times\mathrm{Re}\{\zeta[\epsilon_a(\mathbf{k})+\epsilon_b(\mathbf{k}')-\epsilon_a(|\mathbf{k}+\mathbf{q}|)-\epsilon_b(|\mathbf{k}'-\mathbf{q}|)]\}, \tag{4}$$

$$\Omega_{\mathbf{k}}^{*}|_{\mathrm{CC}}=2\sum_{\substack{\mathbf{k}',\mathbf{q}\\ b=e,h}}|W(\mathbf{q})|^2(f_{\mathbf{k}'-\mathbf{q}}^{b}-f_{\mathbf{k}'}^{b})P_{\mathbf{k}+\mathbf{q}}^{*}\times\zeta^{*}[\epsilon_{\tilde{a}}(\mathbf{k})+\epsilon_b(\mathbf{k}')-\epsilon_{\tilde{a}}(|\mathbf{k}+\mathbf{q}|)-\epsilon_b(|\mathbf{k}'-\mathbf{q}|)], \tag{5}$$

$$Q_{\mathbf{k}}^{*}=2\sum_{\substack{\mathbf{k}',\mathbf{q}\\ b=e,h}}|W(\mathbf{q})|^2(f_{\mathbf{k}}^{a}-f_{\mathbf{k}+\mathbf{q}}^{a})P_{\mathbf{k}'}P_{\mathbf{k}'-\mathbf{q}}^{*}\times\zeta^{*}[\epsilon_a(\mathbf{k})+\epsilon_b(\mathbf{k}')-\epsilon_a(|\mathbf{k}+\mathbf{q}|)-\epsilon_b(|\mathbf{k}'-\mathbf{q}|)] \tag{6}$$

(if $a=h$, then $\tilde{a}=e$ and vice versa), and $\Gamma_{\mathrm{out}}^{a,\mathrm{cc}}$ is obtained by replacing f by $1-f$. The interaction potential W is the screened Coulomb potential, which is treated here in a quasistatical screening model [2] and the ζ function is given by $\zeta(x)=\pi\delta(x)+i\mathcal{P}/x$, where $\mathcal{P}$ denotes the principal value. Similarly, the polarization functions take the form

$$\left.\frac{\partial P_{\mathbf{k}}}{\partial t}\right|_{\mathrm{CC}} = -\Gamma_{\mathrm{d}}^{\mathrm{p,CC}}(\mathbf{k},f\,)P_{\mathbf{k}} + \sum_{\mathbf{q}} \Gamma_{\mathrm{nd}}^{\mathrm{p,CC}}(\mathbf{k},\mathbf{q},f\,)P_{\mathbf{k}+\mathbf{q}}, \tag{7}$$

where the diagonal dephasing rate $\Gamma_d^{p,\mathrm{cc}}$, which accounts for loss of coherence of P_k, can be written

$$\begin{aligned}\Gamma_{\mathrm{d}}^{\mathrm{p,cc}}(\mathbf{k},f\,)P_{\mathbf{k}} = 2 \sum_{\substack{\mathbf{k}',\mathbf{q} \\ b,a=e,h}} |W(\mathbf{q})|^2 [& f^a_{\mathbf{k}+\mathbf{q}}(1-f^b_{\mathbf{k}'}) f^b_{\mathbf{k}'-\mathbf{q}} \\ & + f \leftrightarrow (1-f\,) - P_{\mathbf{k}'} P^*_{\mathbf{k}'-\mathbf{q}}] \zeta[\epsilon_a(\mathbf{k}) + \epsilon_b(\mathbf{k}') \\ & - \epsilon_a(|\mathbf{k}+\mathbf{q}|) - \epsilon_b(|\mathbf{k}'-\mathbf{q}|)],\end{aligned} \tag{8}$$

and the nondiagonal scattering rate

$$\begin{aligned}\Gamma_{\mathrm{nd}}^{\mathrm{p,CC}}(\mathbf{k},\mathbf{q},f\,) = 2 \sum_{\substack{\mathbf{k}' \\ b,a=e,h}} |W(\mathbf{q})|^2 [& f^a_{\mathbf{k}}(1-f^b_{\mathbf{k}'-\mathbf{q}}) f^b_{\mathbf{k}'} \\ & + f \leftrightarrow (1-f\,) - P^*_{\mathbf{k}'} P_{\mathbf{k}'-\mathbf{q}}] \zeta[\epsilon_a(\mathbf{k}) + \epsilon_b(\mathbf{k}') \\ & - \epsilon_a(|\mathbf{k}+\mathbf{q}|) - \epsilon_b(|\mathbf{k}'-\mathbf{q}|)]\end{aligned} \tag{9}$$

describes the rate of polarization transfer between the states k and q due to carrier-carrier scattering [19].

For light propagation studies that take the finite extension of the sample into account, one must describe in additon to the material variables the spatial and temporal evolution of the field E. For simplicity we assume input plane waves of the form $E(\mathbf{r},t)=E(z,t)[\exp(-i\omega_0 t + k_l t) + \mathrm{c.c.}]$. However, for broad-area lasers, large aperture surface-emitting lasers, and SOA's that exhibit dynamical changes in the mode confinement factor [20], complex transverse mode structures may appear and one must also account for the transverse mode dynamics. One might, for example, derive effective Bloch equations (computationally much less intense) from the SBE's [21] using the above equations as an ideal starting point. The subsequent evolution of the electric field envelope in the traveling frame of reference $(\zeta,\eta)=(z,t-zc/n_b)$ (n_b being the background index) can be obtained from the reduced wave equation

$$\frac{\partial E(\zeta,\eta)}{\partial \zeta} = \frac{i\mu_0\omega_0^2\Gamma^2}{k_0 V} \sum_{\mathbf{k}} d_{cv}(k) P_{\mathbf{k}} i C P(t), \tag{10}$$

where the slowly varying envelope approximation has been applied [22,23] and Γ is the waveguide confinement factor.

For all following numerical calculations we choose parameters suitable for bulk GaAs, namely, electron/hole mass ratio $m_e/m_h = 3/7$; excitonic binding frequency $E_x = 4.2$ meV, and exciton Bohr radius $a_0 = 13.5$ nm. The light field is taken to be an intense sech-shaped pulse with an input unrenormalized Rabi energy of 10–50 meV ($\approx 0.5 - 2$ GW cm^{-2}) and of 120 fs full width at half maximum irradiance (FWHM), unless stated otherwise. As an initial condition we assume a quasiequilibrium distribution of the electrons and holes in the valence and conduction bands at room temperature with an incoherent carrier distribution of $N = 3\times 10^{18}$ cm^{-3}. One should note that all discussed nonlinear saturation effects scale somewhat with the initial carrier density, thus the typical saturation intensities decrease if the initial carrier density is reduced and vice versa.

In the field of SOA's, the role of non-Markovian relaxation has been employed to explain the apparent inconsistency of modeling gain spectra with a Lorentzian profile for the interband transition line shape since Lorentzian line shapes yield a certain amount of unphysical absorption below the renormalized band gap, which is not obtained in experiments. Subsequently, for modeling electronic processes within the ultrafast time-scale regime, one may require a kinetic theory beyond the usual Boltzmann kinetics with energy conservation for each of its collisions. In this sense, Ref. [24] demonstrated that non-Markovian processes modify the line shape of semiconductor lasers in such a manner as to calculate no considerable absorption below the renormalized band gap. Little quantitative work has been performed since then and the role of non-Markovain relaxation is still not well established in the field of SOA's. Recently, a phenomenonological memory model has also been proposed [25] (''two-pole approximation'') for calculating non-Markovian line shapes and modeling pulse propagation. The two-pole scheme demonstrates that the phenomenological inclusion of memory effects in the description of dephasing processes reduce the artifacts in the local linear gain spectra brought about by the dephasing-rate approximation. Additionally, in the nonlinear regime, the inclusion of memory effects was seen to significantly affect the dynamical pulse reshaping processes; in particular, the threshold for the saturation of the gain becomes significantly reduced, even for excitation by 150-fs optical pulses.

On the other hand, as shown recently in Ref. [7], if one includes the proper diagonal and nondiagonal dephasing [as above in Eqs. (7) and (8)] for the semiconductor polarization equations, then the line shape obtained at typical gain plasma densities deviates considerably from Lorentzian and no absorption below the renormalized band gap is calculated because of the reduced influence of the higher wave number (absorbing) states, even within the Markov approximation. This, however, does not imply that non-Markovian relaxation processes are not important for estimating the linear gain spectra (or nonlinear processes) of semiconductor lasers. It depends very much on the experimental conditions, the relative time scale of the probing pulse, and the optical amplifier under investigation. The effects of nondiagonal dephasing and non-Markovian relaxation clearly manifest themselves in a similar manner, but since memory times for bulk GaAs have been calculated recently in Ref. [26] to be less than 8 fs we will tacitly ignore the effects of non-Markovian relaxation in this work. Furthermore, recent FWM experiments for the SOA, which could not be explained by the dephasing-rate approximation, were explained well by the inclusion of nondiagonal dephasing in the Markov approximation [10]. We would like to point out, however, that a proper analysis using both non-Markovian and nondiagonal dephasing is highly desirable, though very computationally intense. In a lower-density regime where carrier-carrier scattering is very inefficient, there is strong evidence for non-Markovian relaxation via the electron–LO-phonon scattering in bulk GaAs [27].

To compare the microscopic model with a simple phenomenological model we introduce the relaxation time ap-

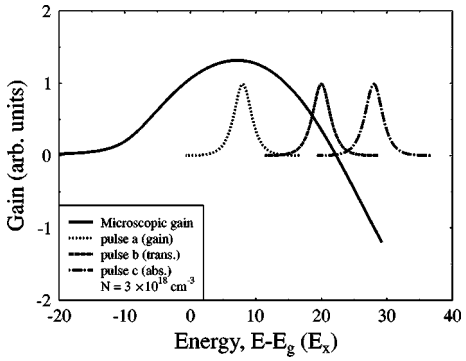

FIG. 1. Gain spectrum for a semiconductor amplifier at room temperature with an incoherent electron-hole density of $N=3\times10^{18}$ cm^{-3}. Also shown are the spectral profiles of the incident pulses ($\tau_p=120$ fs) excited in the gain, transparency, and absorption regimes of the SOA. Energy is in units of excitonic binding energy (E_x).

proximation (RTA) for the Coulomb correlations. The RTA can be derived assuming a simple exponential decay of a small deviation (pulse-induced nonequilibrium carrier distribution) from a quasiequilibrium carrier distribution. Subsequently, the scattering terms for the carrier distribution functions are given by the expression

$$\left.\frac{\partial f_{\mathbf{k}}^{a}}{\partial t}\right|_{\mathrm{CC}} = -\gamma_a^{\mathrm{CC}}[f_{\mathbf{k}}^{a}-F_{\mathbf{k}}(\mu^a,T_{\mathrm{pl}})],$$

where F denotes Fermi functions with chemical potentials μ^a and plasma temperature T_{pl} $(a=e,h)$. The relaxation rate γ_a^{CC} should ideally be evaluated at the spectral region of interest and is k independent as a consequence of carrier conservation. By using the RTA, the plasma temperature has to be computed dynamically because carrier-carrier scattering leaves the total kinetic energy of the carrier system unchanged (for details see Appendix B of Ref. [28]).

Similarly, for the polarization functions $\dot{P}_{\mathbf{k}}|_{\mathrm{CC}}=-\gamma_0^{\mathrm{p}}P_{\mathbf{k}}$, where the total dephasing rate of the optical polarization is $\gamma_0^{\mathrm{p}}=\frac{1}{2}(\gamma_e^{\mathrm{CC}}+\gamma_h^{\mathrm{CC}})$, which in principle can be treated as a fit parameter. Note that within the RTA, the Coulomb potential in the Hartree-Fock terms has to be replaced by the screened Coulomb potential and by the Coulomb hole term to account for some of the carrier correlation effects (see, for example, Ref. [2]).

III. LINEAR GAIN AND PULSE-INDUCED CARRIER HEATING IN THREE SPECTRAL REGIMES

To characterize the investigated amplifier we start with the calculation of the linear gain spectrum. A linear gain spectrum can be measured by transmitting a light field with an initial power spectrum $I_0(\omega)$ through a gain medium, measuring the transmitted spectrum $I(\omega)$, and relating both by the definition of the gain

$$G(\omega)=\frac{1}{z}\ln\frac{I(\omega)}{I_0(\omega)}, \tag{11}$$

where z is the propagation length through the sample.

In Fig. 1 we plot the gain spectrum (solid line) of the considered amplifier versus the detuning of the frequency with respect to the unrenormalized band edge. The prediction of gain spectra using the microscopic theory presented in the preceding section is very accurate; for a comparison with the experiments compare, for instance, Ref. [29]. Clearly, the Coulomb-induced band gap renormalization [see Eq. (2), which contains the renormalized energy dispersion] generates gain below the band edge [22]. For the study of nonlinear gain saturation processes we inject pulses in the gain regime (dotted line), the transparency regime (dashed line), and the absorption regime (chain line) of the SOA. These pulses are respectively termed *a*, *b*, and *c* in the figure.

There are a number of pulse-induced physical mechanisms that may contribute to the optical response measured in SOA's. In the linear regime, for carrier frequencies above the transparency point, absorption creates electron-hole pairs and increases the carrier density. For excitation below the transparency point (gain regime), pulse-stimulated emission reduces the carrier density. At the transparency point, stimulated emission and absorption occur with equal probability and there is only a small net change in density as long as the pulses are spectrally sharp. In the nonlinear regime, the heating of the carrier distributions also have a strong influence on the position of the transparency point and peak gain in the amplifier after the establishment of a quasiequilibrium situation. To have an estimate of the gain dynamics we study the temporal development of the carrier density as well as the time-dependent gain spectrum ''seen'' by a probe pulse.

First we study pulse excitation in the gain region of the SOA (pulse *a* in Fig. 1), where $\omega_l=E_g+8\ E_x$. Figure 2(a) depicts the time-dependent density that includes the scattering contributions [see Eqs. (3) and (8)]. The solid, dashed, and dotted lines correspond to the incident Rabi frequencies of 10, 30, and 50 meV, respectively. With increasing intensity one recognizes the transition from density depletion to saturation, finally arriving at a situation where an instantaneous response around the pulse maximum occurs in the density shape. Gain saturation occurs for increasing irradiances as a consequence of plasma heating, spectral hole burning, and carrier density depletion. Interaction with the light field heats the plasma since the absorption tends to be into high-momentum states, creating hot carriers, and the emission removes carriers from the low-momentum states. Once the plasma is heated, the carriers are distributed across more momentum states and fewer of these states are inverted [compare momentum distribution functions in Fig. 2(b)]. For increasing irradiances an instantaneous nonlinearity that follows the temporal pulse profile is seen [density peak close to zero in Fig. 1(a)]. A numerical analysis shows that the peak occurring at close to zero time results from the interaction of the pulse with off-resonance k states. This interaction is caused by the finite overlap of the pulse and the refractive index profiles of the off-resonance states. Through the virtual excitation by a high peak intensity, the far off-resonance states transiently contribute strongly to the total electron-hole density. The corresponding electron-hole density adiabatically follows the pulse intensity (peak at $t=0$) and hence no real absorption is noticed after the pulse is switched off (scenario of adiabatic following; compare Ref. [30]). Note that the off-resonance states become increasingly important if the resonant states are saturated by the strong optical pulse. To

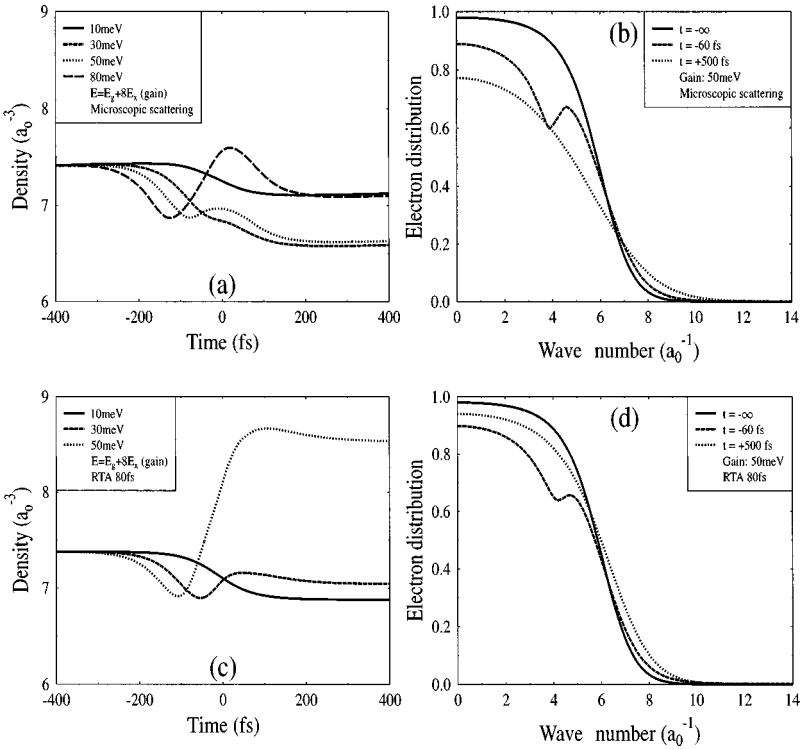

FIG. 2. (a) Temporal behavior of the total electron-hole density for the microscopic scattering processes for excitation in the gain regime of the SOA, $\omega_l = E_g + 8E_x$. The input unrenormalized Rabi energies of 10, 30, 50, and 80 meV are shown, respectively, by the solid, dotted, short-dashed, and long-dashed lines. The wave number is given in units of inverse bohr radius (a_0^{-1}). (b) Distribution of electrons at various snapshots in time with microscopic scattering, corresponding to the density shown in (a) at 50 meV (gain regime). (c) Same as in (a), but by employing a relaxation-time-approximation (RTA) dephasing time of 80 fs. (d) Same as in (b), but with the RTA time of 80 fs, corresponding to the density shown in (c) at 50 meV.

illustrate the form of the action of adiabatic following more clearly, in Fig. 2(a) the effect is emphasized by including the higher irradiance run of 80 meV, which exhibits a clear instantaneous (Kerr nonlinearity; see below) nonlinearity around the center of the pulse.

We have also studied pulse-excitation dynamics by employing the relaxation-time approximation for $T_1 = T_2 = 80$ fs ($1/\gamma_a^{CC} = 1/\gamma_0^{p} = 80$ fs); this RTA time corresponds closely to the calculated value for GaAs optical amplifiers presented in Ref. [28]. From Fig. 2(c) the RTA simulation for weak intensities demonstrates a decrease of the density change, as expected since the linewidths of the absorbing k states are increased by the application of the RTA (nondiagonal dephasing not accounted for). For higher intensities, if the inverted states are saturated, the dynamics become dominated by the absorbing states and the density increases even above the initial level. Further, we have also numerically verified that by choosing a longer RTA time the microscopic density responses are still not captured and even exhibit very small oscillations in the density profiles for the higher irradiances (30 and 50 meV). These oscillations are due to Rabi oscillations in the density, which are not present in the microscopic description. Thus we can conclude that there is no RTA time that can accurately capture all the dynamics of the microscopic response, although, the RTA simulation at 30 meV is somewhat similar to the 50-meV microscopic simulation, but does not, however, capture the decrease in density after the pulse maximum. Additionally, there is undeniable evidence for adiabatic following in the microscopic dephasing calculations.

To investigate the microscopic origin for the temporal density dependence, we plot the distribution function f_k for different times, i.e., before, during, and after the incident pulse. Before the pulse, the electron and hole distributions both have the shape of Fermi-Dirac functions, with the corresponding temperature agreeing with that of the lattice (300 K). During the pulse the carrier distributions are in a highly nonequilibrium state and hole burning is observed [see Figs. 2(b) and 2(d)]. Absorption into high-lying k states with above average kinetic energy results in a heating of the distribution that corresponds to gain saturation. This effect has been discussed in detail elsewhere [31]. The microscopic treatment of the scattering mechanisms show that contributions from carrier-carrier scattering reduce the interband optical linewidths of the higher k states and decrease the spectral overlap of absorbing states with the spectral pulse shape, which results in a reduction of the occupation in comparison to the RTA treatment; compare Figs. 2(b) and 2(d). As discussed in Sec. II, it is this reduction of the electron-hole optical linewidths that enabled us to calculate a realistic gain spectum. By employing the RTA, absorption occurs below the band gap in the gain spectrum, which is not, however, observed in experiments [22]; for a detailed discussion, see Ref. [32]. The resulting highly non-Lorentzian line shapes are a manifestation of the self-consistent inclusion of nondiagonal dephasing. We emphasize that our self-consistent microscopic approach results in strongly time-dependent and energy-dependent dephasing rates. For that reason, absorp-

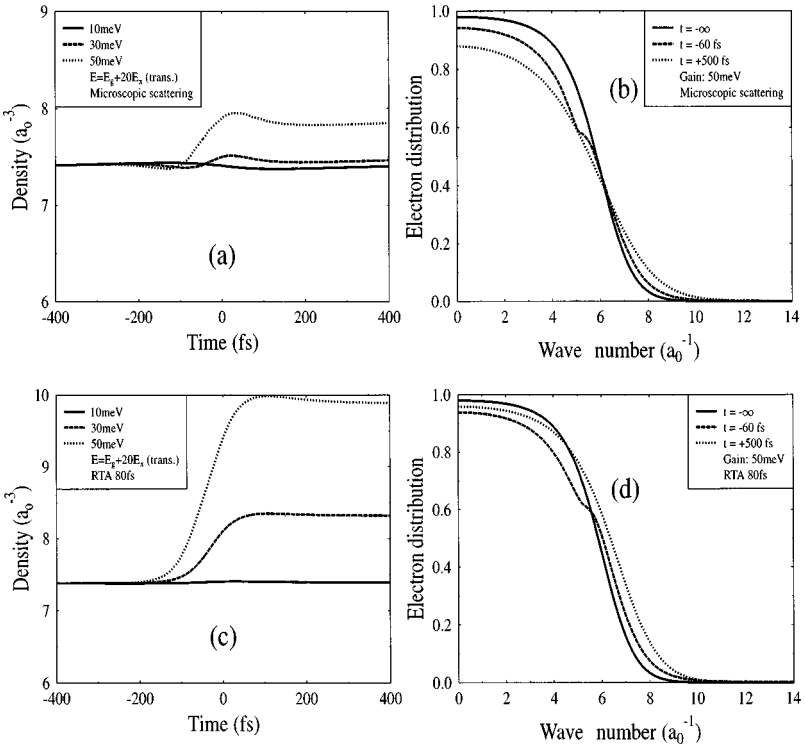

FIG. 3. (a) Temporal behavior of the total electron-hole density for the microscopic scattering processes for excitation in the transparency regime of the SOA, $\omega_l = E_g + 20E_x$. The input Rabi frequencies of 10, 30, and 50 meV are shown, respectively, by the solid, dotted, and dashed lines. (b) Distribution of holes at various snapshots in time with microscopic scattering, corresponding to the density shown in (a) at 50 meV (transparency regime). (c) Same as in (a), but by employing the RTA dephasing time of 80 fs. (d) Same as in (b), but with the RTA time of 80 fs, corresponding to the density shown in (c) at 50 meV.

tion processes taking place from the high-wave-number regime are reduced and the final density decreases accordingly. This can be recognized by comparing the final Fermi distributions of the RTA simulations and microscopic scattering cases, shown in Figs. 2(b) and 2(d). Several other works [24,25,33] have also pointed out that the inconsistencies arising from the neglect of nondiagonal dephasing can be partially accounted for by including a frequency-dependent dephasing of the optical polarization or by the inclusion of non-Markovian relaxation (see Sec. II).

Now we investigate the situation where the carrier frequency of the pulse is injected at the transparency point of the SOA, with $\omega_l = E_g + 20E_x$ (see Fig. 1). For pulse excitation near transparency, the effects of stimulated emission and absorption approximately cancel each other, at least in a spectrally narrow region. Figure 3(a) depicts the net density at the front facet of the amplifier as a function of time. Saturation of the gain is much easier to achieve because we are exciting near the transparency regime and more hot carriers can be created. It can be recognized, again, that for high irradiances adiabatic following from the off-resonance states occurs. The effects of adiabatic following are much weaker in comparison to excitation in the gain regime and now only a small instantaneous nonlinearity is seen for the higher irradiance pulse (50 meV, dotted line).

In Fig. 3(c) we plot the RTA results for relaxation times of 80 fs [34]. While the RTA simulations do not predict any instantaneous transient effects around zero (and obtain greater density changes), simulations with longer lifetimes can help obtain slight instantaneous contributions for increasing irradiances and smaller net density changes. In this case, Rabi oscillations do not occur for longer RTA times because the reduced Pauli blocking is very ineffective at the transparency point. Consequently, we predict that for low and intermediate pulse irradiances, the RTA may, with care, be successfully applied provided one chooses the appropriate time constant. The corresponding electron distributions for the higher irradiance cases are depicted in Figs. 3(b) and 3(d) and show features similar to those for excitation at the gain peak; however, spectral hole burning is strongly suppressed.

Next we study the situation where the carrier frequency of the input pulse is in the absorption regime of the SOA, with $\omega_l = E_g + 28E_x$ (see Fig. 1). At this excitation frequency, the pulse spectrum lies fully inside the absorption region. Thus via the injected pulse, stimulated electron-hole pairs increase the carrier density. Figure 4(a) illustrates the time evolution of the density as a function of time, which includes the microscopic scattering processes. As expected, for energies above the transparency point, the pulse experiences absorption and therefore increases the carrier density. From the figure we see that the influence of adiabatic following at these irradiances is negligible as we are exciting higher above the band gap. In this case, the RTA simulations of 80 fs [Fig. 4(c)] reproduce the microscopic density responses considerably better than the previous cases, although the final densities are still too high. However, RTA simulations with longer lifetimes will yield very similar results to the microscopic calculations showing the RTA to be reasonable in this regime. The corresponding electron distribution func-

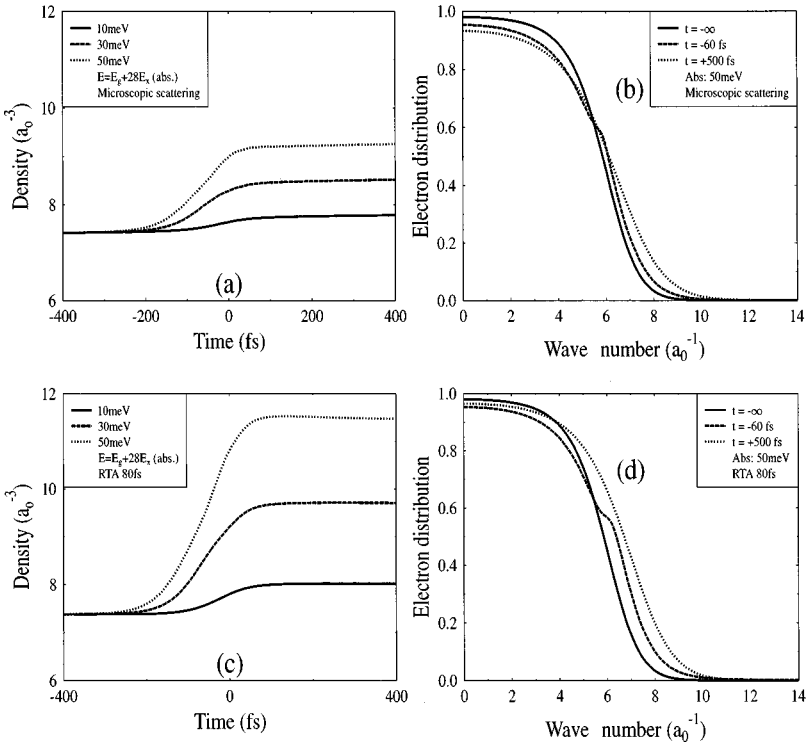

FIG. 4. (a) Temporal behavior of the total electron-hole density for the microscopic scattering processes for excitation in the absorption regime of the SOA, $\omega_l = E_g + 28E_x$. The input unrenormalized Rabi frequencies of 10, 30, and 50 meV are shown, respectively, by the solid, dotted, and dashed lines. (b) Distribution of electrons at various snapshots in time with microscopic scattering, corresponding to the density shown in (a) at 50 meV (absorption regime). (c) Same as in (a), but by employing the RTA dephasing time of 80 fs. (d) Same as in (b), but with the RTA time of 80 fs, corresponding to the density shown in (c) at 50 meV.

tions for the higher irradiance study are shown in Figs. 4(b) and 4(d). Spectral hole burning occurs, but, as expected, is much less pronounced for excitation in the higher spectral regions. Significant heating also takes place, primarily due to the creation of hot carriers (in the high-momentum states). However, in this case, there is no evidence for adiabatic following because of the very weak saturation of the resonant states.

Before closing this section we would like to briefly point out that all the above effects can be obtained qualitatively by replacing the Coulomb potentials in the Hartree-Fock calculations by the standard screened potentials and Coulomb hole self-energies. One may then calculate the scattering integrals using a δ-function approximation and the numerics become considerably easier (three-dimensional instead of four-dimensional integration). However, the real parts of the self-energies can give rise to a shift in the gain [35] and for a more detailed investigation, the real parts of the self-energies and indeed the inclusion of non-Markovian relaxation may be required.

IV. COMPARISON WITH EXPERIMENTS AND THE ROLE OF ADIABATIC FOLLOWING

In all three excitation regimes of the SOA (gain, transparency, and absorption) the Fermi distributions are smeared out due to carrier heating and this significantly reduces the gain on a femtosecond time scale. Further, instantaneous nonlin-

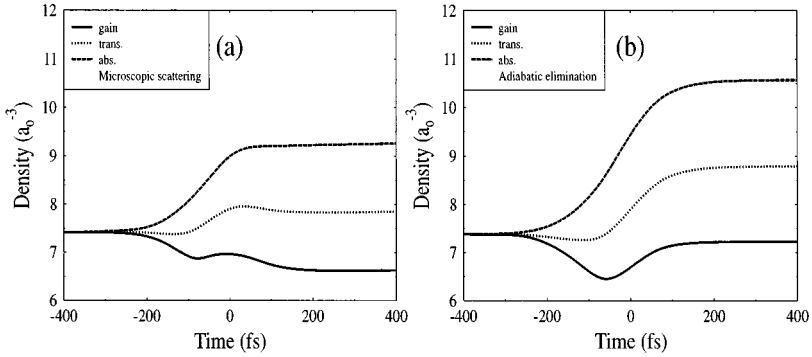

FIG. 5. (a) Temporal behavior of the total electron-hole density for the microscopic scattering processes for excitation in the gain (solid line), transparency (dotted line), and absorption regime (dashed line) of the SOA. The input Rabi energy was 50 meV. (b) Same as in (a), but by employing an adiabatic elimination for the polarization equation (see the text).

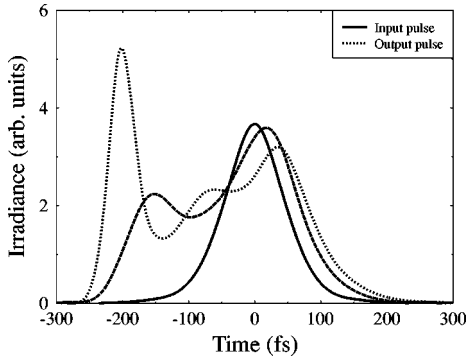

FIG. 6. Pulse irradiance profiles for propagation through the semiconductor amplifier at the gain peak; strong pulse reshaping occurs as a manifestaion of amplification and adiabatic following (see the text).

earities around the center of the pulse are evident for pulse excitation in the gain and transparency regimes of the SOA due to the effects of adiabatic following from the off-resonance states, which can be viewed as a Kerr-like nonlinearity. Our calculations show that under high-excitation conditions the adiabatic following may overcompensate for amplification and gain saturation. The nonlinearity introduced by the adiabatic following process is a typical Kerr nonlinearity: $P \sim E|E|^2$. This Kerr-type effect is formally identical to the action of a TPA polarization source in the wave equation (see, for example, Ref. [36], where it was also noted that the same effect in the rate equation approach could be obtained by including any Kerr-type nonlinearity). For our chosen laser and semiconductor parameters we do not predict any instantaneous nonlinearity above transparency. Because we can relate the action of the instantaneous nonlinearity with the pulse shape change of a propagating pulse (compare Sec. VII) we can compare these predictions with the experiment, presented in Ref. [12]. The predicted instantaneous nonlinearities that act during the pulse propagation are in complete agreement for all three excitation regimes; i.e., for sub-picosecond pulse propagation in SOA's a strong pulse shoulder develops in the gain regime (see Sec. VI), a small shoulder occurs in the transparency regime, and no significant pulse reshaping takes place in the absorption regime.

On the other hand, from pump-probe–type experiments [4], there is a strong instantaneous nonlinearity for pulse excitation in the gain regime of the amplifier. For weaker intensities the instantaneous effects disappear in pump-probe experiments [37]. This intensity dependence could be explained by the adiabatic following investigated here. However, there is also evidence for an instantaneous nonlinearity above transparency, which is not predicted within the presented theory. Measurements indicate that this nonlinearity is highly probe polarization sensitive [38], which may be due to coherent coupling artifacts (see, for example, Ref. [39]) or wave mixing beween the pump and probe fields or other nonlinearities such as TPA or FCA. However, we conclude that for high intensities the intrinsic nonlinearities in a semiconductor such as adiabatic following should not be neglected because they clearly contribute to the optical response.

V. POLARIZATION DYNAMICS AND THE ADIABATIC APPROXIMATION

In the phenomenological description of gain nonlinearities it is often assumed that the dynamics of the polarization can be adiabatically eliminated (adiabatic approximation), even on a femtosecond time scale (see, for example, Refs. [36, 40]). This procedure implies that the polarization decay time is much smaller than the time scale for which the population or the electric field changes. From the preceding discussion we know that within a microscopic description, distribution functions and the polarization are strongly connected and that dephasing and relaxation primarily occur via carrier-carrier interactions. Therefore, it is not *a priori* clear that one can really apply the adiabatic approximation quantitatively. However, within the microscopic description presented here we can investigate the validity of the adiabatic approximation. For this purpose, we compare the pulse-induced density in the transparency, absorption, and gain regimes of the SOA with an input Rabi energy of 50 meV and compare directly to the ''adiabatic elimination'' scenario, which assumes that the rate of change of the polarization components is zero (with respect to any other changes); i.e., we set the left-hand side of Eq. (2) equal to zero and substitute the resulting adiabatic solution directly into Eq. (1) (for the carrier distributions), which is solved numerically as before. Figures 5(a) and 5(b) compare the two situations and as can be clearly discerned, the adiabatic elimination calculations do not capture the nonlinearities around (and after) the center of the pulse, which are caused by the microscopic scattering processes. Thus we conclude that, in general, in order to properly account for the nonlinear changes around (and after) the center of the pulse, one cannot invoke an adiabatic elimination of the polarization. Furthermore, for excitation near the transparency regime, coherent effects and a frequency-dependent refractive index are required, even in the linear regime [14,15]. Both requirements are not captured by the adiabatic elimination procedure for the polarization.

VI. PULSE PROPAGATION AT THE GAIN PEAK

Most SOA's are extended samples where light propation effects cannot be neglected. To investigate the major impact of the nonlinear gain dynamics on pulse propagation we study the temporal shape of a pulse at the peak gain of the optical amplifier by solving the SBE's self-consistently with the wave equation (see Sec. II). The initial pulse is chosen to be sech shaped with an input Rabi energy of 50 meV and a pulse duration of 100 fs (FWHM). The carrier frequency of the pulse coincides with the gain maximum and the pulse spectrum lies fully inside the gain region. In Fig. 6 we plot the correponding pulse as it propagates through the amplifier. Strong pulse reshaping is seen over a propagation length of several hundred micrometers (dashed line, 120 μm; dotted line, 200 μm). It can be recognized that a shoulder develops near the initial part of the pulse (pulse broadening), which eventually splits off from the main part of the pulse. The reason for the reshaping is that for high-intensity pulses, gain saturation and adiabatic following overcompensate for the amplification. The propagation-induced reshaping mechanism results from a change in the electron density [compare Fig. 2(a)]. The leading edge of the pulse is amplified (de-

creasing density), whereas the onset of adiabatic following absorbs the pulse (increasing density). Therefore, the leading part of the pulse grows in suspense of the trailing part. Thus the interplay of different microscopic mechanisms results in the development of nontrivial pulse shapes, which in principle yield the microscopic limits for applications of semiconductor lasers and amplifiers for short pulse generation and amplification. Experimentally [12], the femtosecond propagation measurements in the gain regime of a SOA are very similar to our intermediate pulse-propagation scenario (dashed line). Also in the experimental measurements, as discussed above, only a small shoulder occurs in the transparency regime and no significant pulse reshaping takes place in the absorption regime. These excitation regimes are consistent with our theoretical findings; i.e., a strong instantaneous nonlinearity occurs for pulse excitation in the gain regime of the SOA, but no instantaneous nonlinearity is expected for excitation above the transparency point.

VII. CONCLUSIONS

In conclusion, we have studied femtosecond pulse-induced density, gain, and propagation dynamics of a semiconductor amplifier within the framework of the semiconductor Maxwell-Bloch equations. We have shown that basic semiconductor nonlinearities such as carrier heating, gain saturation, and adiabatic following can be described within a parameter-free microscopic theory and may significantly contribute to the optical response of SOA's. For increasing intensity, the temporal density profiles show a significant adiabatic following process that can be phenomenologically attributed to a Kerr-type nonlinearity. Moreover, we have demonstrated that an adiabatic elimination of the polarization often done in rate equation theories is not valid on femtosecond time scales. Pulse propagation at the gain peak shows strong pulse reshaping as a result of the competition of amplification and adiabatic following in the SOA. Many of our results are consistent with experimental observations and show that for the SOA, a treatment of coherent and incoherent effects on the level of a microscopic theory is both timely and highly desirable to enable the rate equation approaches to transcend to a more sophisticated level.

ACKNOWLEDGMENTS

The author thanks the Japanese Society for the Promotion of Science, the National Science Foundation, and the Office of Naval Research, for partial financial support. Andreas Knorr and Stephan W. Koch, Phillips Universität, Marburg, Germany, are acknowledged for many insightful discussions.

[1] For a textbook discussion see G. A. Agrawal and N. K. Dutta, *Long-Wavelength Semiconductor Lasers* (Springer, Berlin, 1986); *Quantum Well Lasers*, edited by P. Zory (Academic, New York, 1993); S. Nakamura amd G. Farol, *The Blue Laser Diode* (Spinger-Verlag, Berlin, 1997). For a recent review see H. Luo and J. K. Furdyna, Semicond. Sci. Technol. **10**, 1041 (1995); S. Nakamura, Solid State Commun. **102**, 237 (1997).

[2] For a textbook discussion see H. Haug and S. W. Koch, *Quantum Theory of the Optical and Electronic Properties of Semiconductors*, 3rd ed. (World Scientific, Singapore, 1994).

[3] See, for example, M. S. Stix, M. P. Kesler, and E. P. Ippen, Appl. Phys. Lett. **48**, 1722 (1986); C.-K. Sun, H. K. Choi, C. A. Wang, and J. G. Fujuimoto, *ibid.* **62**, 747 (1993).

[4] See, for example, J. Mark and J. Mørk, Appl. Phys. Lett. **61**, 2281 (1992); C. T. Hultgren, D. J. Dougherty, and E. P. Ippen, *ibid.* **61**, 2767 (1992); K. Hall, G. Lenz, E. P. Ippen, U. Koren, and G. Raybon, *ibid.* **61**, 2512 (1992); J. Mørk, J. Mark, and C. P. Seltzer, *ibid.* **64**, 2206 (1994).

[5] See, for example, A. D'ottiva, E. Iannone, A. Mecozzi, S. Scotti, P. Spano, J. Landreau, A. Ougazzaden, and J. C. Bouley, Appl. Phys. Lett. **64**, 2492 (1994); L. F. Tiemeinijer, *ibid.* **59**, 499 (1991); J. Zhou, N. Park, J. W. Dawson, K. J. Vahala, M. A. Newkirk, and B. I. Miller, *ibid.* **63**, 1179 (1993).

[6] F. Jahnke and S. W. Koch, Phys. Rev. A **52**, 1712 (1995).

[7] A. Knorr, S. Hughes, T. Stroucken, and S. W. Koch, J. Chem. Phys. **210**, 27 (1996); S. Hughes, A. Knorr, and S. W. Koch, J. Opt. Soc. Am. B **14**, 754 (1997).

[8] M. F. Pereira and K. Henneberger, Phys. Rev. B **53**, 16 485 (1996).

[9] M. Hofmann, S. D. Brörson, J. Mørk, and A. Mecozzi, Appl. Phys. Lett. **68**, 3236 (1996).

[10] S. Hughes, Opt. Lett. **23**, 948 (1998).

[11] S. Jiang and L. W. Casperson, J. Appl. Phys. **73**, 530 (1993).

[12] Y.-H. Kao, I. V. Goltser, M. Jiang, M. N. Isla, and G. Raybon (unpublished).

[13] R. Indik, A. Knorr, R. Binder, J. Moloney, and S. W. Koch, Opt. Lett. **19**, 966 (1994).

[14] S. Hughes, A. Knorr, and S. W. Koch, Opt. Lett. **21**, 1052 (1996).

[15] Y.-H. Kao, I. V. Goltser, M. Jiang, and M. N. Islam, Appl. Phys. Lett. **69**, 4227 (1996).

[16] M. Lindberg and S. W. Koch, Phys. Rev. B **38**, 3342 (1988).

[17] T. Rappen, U.-G Peter, M. Wegener, and W. Schäfer, Phys. Rev. B **49**, 10 774 (1994).

[18] F. Rossi, S. Haas, and T. Kuhn, Phys. Rev. B **53**, 12 855 (1996).

[19] Note that the Coulomb exchange in the scattering terms are neglected here since for our studies only a small reduction of the overall dephasing rate would take place, changing the results quantitatively but not qualitatively.

[20] D. Botkin, S. Weiss, G. Sucha, D. S. Chemla, and J. M. Wiesenfeld, Appl. Phys. Lett. **64**, 2861 (1993).

[21] C. Z. Ning, R. A. Indik, and J. V. Moloney, IEEE J. Quantum Electron. **33**, 1543 (1997).

[22] For a textbook discussion see W. W. Chow, S. W. Koch, and M. Sargent. III, *Semiconductor-Laser Physics* (Springer, Berlin, 1994).

[23] A. Knorr, R. Binder, M. Lindberg, and S. W. Koch, Phys. Rev. A **46**, 7179 (1992).

[24] M. Yamanishi and Y. Lee, IEEE J. Quantum Electron. **QE-14**, 367 (1987); T. Ohtoshi and M. Yamanishi, *ibid.* **27**, 46 (1991).

[25] R. A. Indik, M. Mlejnek, J. V. Moloney, R. Binder, S. Hughes, A. Knorr, and S. W. Koch, Phys. Rev. A **53**, 3614 (1996).

[26] S. Hughes, Solid State Commun. **104**, 107 (1997).

[27] See, for example, C. Fürst, A. Leitenstorfer, A. Laubereau, and R. Zimmermann, Phys. Rev. Lett. **78**, 3733 (1997); M. U. Wehner, M. H. Ulm, D. S. Chemla, and M. Wegener, *ibid.* **80**, 1992 (1998).
[28] R. Binder, D. C. Scott, A. E. Paul, M. Lindberg, K. Henneberger, and S. W. Koch, Phys. Rev. B **45**, 1107 (1992).
[29] P. Rees and P. Blood, IEEE J. Quantum Electron. **31**, 31 (1995).
[30] L. Allen and J. H. Eberly, *Optical Resonance and Two-Level Atoms* (Wiley, New York, 1995).
[31] A. Knorr, R. Binder, E. Wright, and S. Koch, Opt. Lett. **18**, 1538 (1993).
[32] S. Hughes, A. Knorr, S. W. Koch, R. Binder, R. A. Indik, and J. V. Moloney, Solid State Commun. **100**, 555 (1996).
[33] D. Ahn, Phys. Rev. B **51**, 2159 (1995); P. Rees and P. Blood, Semicond. Sci. Technol. **10**, 1545 (1995); M. F. Pereira and K. Henneberger, Phys. Status Solidi B **202**, 751 (1997).
[34] Note that the transparency point for the microscopic calculations and the RTA simulations differ somewhat because they yield different optical dephasing rates; in addition, the microscopic dephasing processes manifest in highly non-Lorentzian interband line shapes.
[35] A. Girndt, F. Jahnke, A. Knorr, S. W. Koch, and W. W. Chow, Phys. Status Solidi B **202**, 725 (1997).
[36] J. Mørk and A. Mecozzi, Appl. Phys. Lett. **65**, 1737 (1994).
[37] M. P. Kesler and E. P. Ippen, Appl. Phys. Lett. **51**, 1765 (1987).
[38] K. L. Hall, G. Lenz, A. M. Darwish, and E. P. Ippen, Opt. Commun. **111**, 589 (1994).
[39] A. Girndt, A. Knorr, M. Hofmann, and S. W. Koch, J. Appl. Phys. **78**, 2146 (1995).
[40] B. N. Gomatam and A. P. DeFonzo, IEEE J. Quantum Electron. **26**, 1689 (1990); A. Uskov, J. Mørk, and J. Mark, IEEE Photonics Technol. Lett. **4**, 443 (1992); N. Ogasawara and R. Ito, Jpn. J. Appl. Phys., Part 1 **27**, 615 (1988).